In Vivo Analysis of the Electron Transfer within Photosystem I: Are the Two Phylloquinones Involved?†

Pierre Joliot* and Anne Joliot

Institut de Biologie Physico-Chimique, CNRS UPR 1261, 13 rue Pierre-et-Marie Curie, 75005 Paris, France

Received April 13, 1999; Revised Manuscript Received June 9, 1999

ABSTRACT: Electron transfer within PS I reaction centers has been analyzed in vivo in a mutant of *Chlorella sorokiniana* which lacks most of the PS II and of the peripheric antennae, using a new spectrophotometric technique with a time resolution of ∼5 ns. Absorption changes associated with the oxidation of semiphylloquinone (acceptor A_1^-) have been characterized in the 371−545 nm spectral range. The oxidation of A_1^- and the reduction of an iron−sulfur cluster (F_X, F_AF_B) is monitored by an absorption decrease at 377 nm (semiphylloquinone absorption band) and by the decrease of two positive absorption bands around 480 and 515 nm, respectively, very likely associated with a local electrochromic shift induced by A_1^- on a carotenoid molecule localized in its vicinity. A_1^- undergoes a two-phase oxidation of about equal amplitude with half-times of ∼18 and ∼160 ns, respectively. Two hypotheses are proposed to interpret these data: (1) Photosystem I reaction centers are present under two conformational states which differ by the reoxidation rate of A_1^-. (2) The two phylloquinones corresponding to the two branches of the PS I heterodimer are involved in the electron transfer. The similar amplitude of the two phases implies that the rates of electron transfer from P700 to each of the phylloquinones are about equal. The two different rate constants measured for A_1^- oxidation suggests some asymmetry in the relative position of the two phylloquinones with respect to F_X.

PS[1] I complex is present in all oxygen-evolving organisms and catalyzes the electron transfer from plastocyanin to ferredoxin (see reviews in refs *1* and *2*). PS I includes 3 major polypeptides: two transmembrane polypeptides PsaA and PsaB, which form a heterodimer and an extrinsic polypeptide PsaC, located on the stromal side of the complex. Upon excitation of the PS I primary donor P700, an electron is transferred to the primary acceptor A_0 (chlorophyll *a*) and then to a secondary acceptor A_1, identified as a phylloquinone. Photovoltage measurements yield a half-time of 50 ps for the A_0 to A_1 electron-transfer reaction (*3*). One electron is transferred from A_1^- to F_X, an iron−sulfur cluster localized at a central position in the heterodimer. P700, A_0, A_1, and F_X are associated with the PsaA and PsaB polypeptides (see review in ref *4*).

The kinetics of A_1^- oxidation, most generally studied in purifed PS I centers, remains a subject of controversy. Spectroscopic analysis of A_1^- has been performed in the near UV (370−380 nm), i.e., in the absorption band of semiphylloquinone (*5*). Oxidation of A_1^- with a half-time of 15 ns has been reported in PS I centers extracted from spinach chloroplasts (*5*). On the other hand, using a cyanobacterial PS I complex, Brettel (*6*) reported a half-time of 200 ns for A_1^- oxidation. In PS I centers isolated from spinach, Sétif and Brettel (*7*) observed a two-phase oxidation of A_1^- with half-times of 25 and 150 ns, respectively, the relative amplitude of which depends on the preparation procedure. In a recent paper (*8*), Brettel observed a biphasic oxidation of A_1^- in PS I centers isolated from *Synechocystis*, with a half-time of ∼7 ns for the faster component. In the case of spinach and cyanobacterial PS I complexes, Bock et al. (*9*) have measured on the basis of EPR measurements an oxidation time of A_1^- of ∼260 ns. Owing to the time resolution of the method (∼50 ns), the contribution of a faster component is not excluded. By measuring the photoelectric response of oriented PS I membranes, Leibl et al. (*10*) observed a 220 ns rising phase of the membrane potential they ascribed to the electron transfer from A_1^- to F_X, F_A, or F_B iron−sulfur clusters. A selective extraction of F_A and F_B (called here F_AF_B) yields to a loss of about half of the ns phase together with a slight acceleration ($t_{1/2}$ ∼ 170 ns). Sétif and Brettel (*7*) have suggested that a low equilibrium constant for the electron transfer between A_1^- and F_X could explain the biphasic oxidation of A_1^-. In this hypothesis, the fast phase (∼7 or ∼20 ns) is ascribed to a fast redox equilibration occurring between A_1 and F_X while the slower phase (150−200 ns) is associated with the electron transfer from F_X to the iron−sulfur clusters F_AF_B included in the extrinsic PsaC polypeptide.

In this paper, we analyze the kinetics of oxidation of A_1^- following saturating or subsaturating-flash excitation of *Chlorella sorokiniana* whole cells, i.e., with PS I centers unperturbed by any process of extraction or purification. In anaerobic conditions, the PS I charge separation occurs in

† This work is supported by the Centre National de la Recherche Scientifique. The spectrophotometric equipment was built with the financial support of ULTIMATECH (Programme Optique).

* Corresponding author. E-mail: ajoliot@ibpc.fr. Fax: (33) 1 46 33 43 03.

[1] Abbreviations: A_0, primary acceptor (chlorophyll *a* monomer); A_1, secondary acceptor (phylloquinone); FCCP, carbonyl cyanide (4-(trifluoromethoxy)phenyl)hydrazone; F_X, F_A, F_B, and F_AF_B, iron−sulfur clusters included in photosystem I centers; PS, photosystem; P700, photosystem I primary donor.

10.1021/bi990857c CCC: $18.00
Published on Web 07/31/1999

the presence of a large permanent transmembrane potential induced by the hydrolysis of ATP formed by a fermentation process and which can be collapsed by the addition of uncouplers (*11*, *12*). We are thus able to analyze the effect of the delocalized membrane potential on the kinetics of A_1^- oxidation. The high signal-to-noise ratio and the time resolution of our new technique (5−10 ns) allows a characterization of the spectra of the different kinetics components associated with A_1^- oxidation, with a better accuracy than that obtained using purified complexes and conventional spectrophotometers.

MATERIALS AND METHODS

Most of the experiments have been performed using S52 or S8 mutant strains of *Chlorella sorokiniana* isolated by Bennoun and characterized in ref *13*. S52 is a double mutant which lacks PS II and most of the chlorophyll antenna content. The S8 mutant strain we used includes a small amount of PS II centers and a normal chlorophyll antenna. The algae were suspended in 20 mM Hepes buffer, pH 7.2, and 15% ficoll. Experiments were performed after anaerobic incubation for more than 30 min. We have checked that the quinone acceptors associated with the small amount of PS II present in the S8 strain we used was fully reduced in these conditions.

Spectrophotometric measurements were performed using a new home-built apparatus (*14*, *15*), in which the absorption is sampled by weak monochromatic flashes (1 nm bandwidth). A Nd:Yag-pumped optical parametric oscillator (Spectra-Physics MOPO 710) provides these monochromatic flashes at wavelengths continuously tunable from 415 to 650 nm. An additional device (Spectra-Physics Frequency Doubleur FDO 900) provides flashes in the 371−430 nm range. Actinic flashes (6 mJ, 700 nm) are provided by a dye laser pumped by the second harmonic of a Nd:Yag laser (532 nm). At this wavelength of excitation, the illumination of the sample is homogeneous. The total duration of actinic or detecting flashes is about 6 ns. Detecting flashes are fired with a delay (T_d) with respect to the actinic flash tunable from 0 to 100 s with a minimum 5 ns step. The jitter between the actinic and detecting flashes is lower than 1 ns. To take into account some possible drift of T_d, the delay $T_d = 0$ corresponding to the synchronization of the detecting and actinic flashes is determined during the course of an experiment, as follow: the photoinduced absorption change is measured at 430 nm, the absorption peak of P700, upon excitation by subsaturating flashes hitting ∼30% of PS I centers. When the actinic and the detecting flashes are synchronized ($T_d = 0$), half of the photons of the detecting flash probe reaction centers which have not yet been excited by the actinic flash and the amplitude of the absorption change is about half of its maximum value. At 430 nm, the maximum amplitude of the signal is reached for a time $T_d = 5-6$ ns. During the course of an experiment (several hours), the drift of T_d is most generally negligible. We estimate that the indetermination on T_d is less than ±1 ns. Upon a saturating-flash excitation, the full oxidation of P700 is completed before the end of the actinic flash and we estimate that the time delay $T_d = 0$ is shifted by about 2 ns toward negative values compared to a subsaturating-flash excitation. Upon saturating-flash excitation, we observe small absorption changes, not associated with electron transfer reactions within PS I centers and the amplitude of which increase nonlinearly as a function of the flash energy. These absorption changes are short-lived and become negligible for $T_d > \sim 6$ ns.

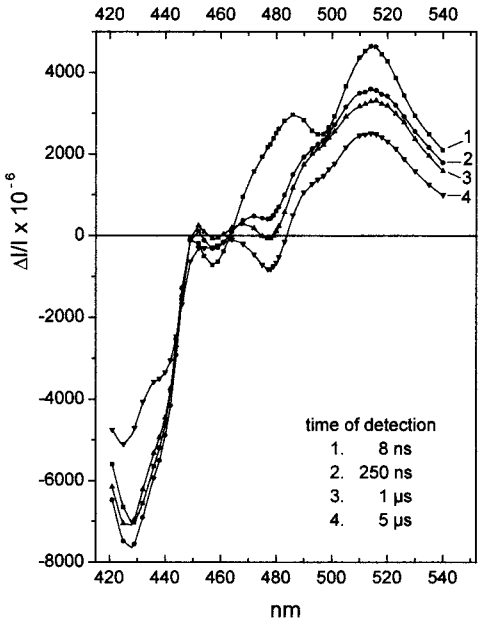

FIGURE 1: Time-resolved flash-induced spectra of S52 mutant: saturating flashes, 0.9 s apart; 8 μM FCCP.

Time-resolved spectra have been analyzed according to a program mexfit (*16*, *17*), which allows the determination of spectra of the different kinetics components, assuming a multiexponential deconvolution of the data.

RESULTS

In Figure 1 are shown time-resolved spectra measured at 8 ns, 250 ns, 1 μs, and 5 μs, respectively, after repetitive saturating-flash excitation of S52 mutant strain of *Chlorella sorokiniana*. The main absorption change, which is associated with the oxidation of P700, peaks around 430 nm and decays within several microseconds.

In Figure 2, spectrum 1 shows the difference between the spectra recorded at 8 ns and 1 μs (Figure 1). Brettel (*6*) suggested that the absorption changes observed in the 450−500 nm range could be associated with the electrochromic shift of a carotenoid pigment, induced by the negatively charged semiphylloquinone. In agreement with this hypothesis, spectrum 1, which displays two positive peaks at 480 and 512 nm and two negative peaks at 457 and 498 nm, resembles the first derivative of a carotenoid absorption spectrum. The small shoulder we observe around 478 nm suggests that the 480 nm absorption band is a double peak. This feature is reproducible and illustrates the high signal-to-noise ratio of the technique. Spectrum 2 displays the spectrum of the delocalized membrane potential. In S52 mutant, which lacks most of chlorophyll antenna, this spectrum is mainly associated with electrochromic shifts of carotenoid pigments different from that involved in spectrum 1, as illustrated by the strong difference between the two spectra.

In Figures 3 and 4, the kinetics of absorption changes have been measured at different wavelengths ranging from 423 to 500 nm. The data have been analyzed using the program

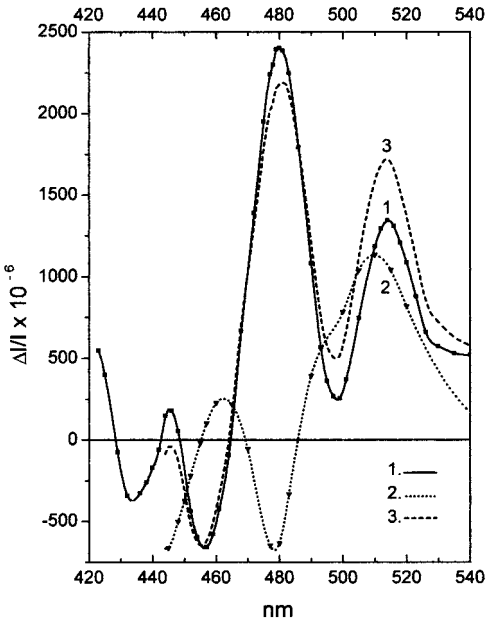

FIGURE 2: Absorption changes associated with the localized or delocalized electrochromic effects of S52 mutant. Spectrum 1 (solid line): difference (8 ns−1 μs) from data Figure 1. Spectrum 2 (dotted line): spectrum of the electrochromic shifts associated with the flash-induced delocalized membrane potential. Spectrum 2 has been measured 50 ms after the flash and normalized to the value of the membrane potential measured at 100 μs. At 50 ms, there is no absorption changes associated with cytochrome *f* or cytochrome *b* redox changes. Spectrum 3 (dashed line): spectrum 1 after correction for the increase of the delocalized membrane potential. The membrane potential rise between 8 ns and 1 μs has been measured in S8 mutant. We have checked that the kinetics of A_1^- oxidation, measured by the difference (481−457 nm) in S8 mutant, is similar to that measured in S52 mutant.

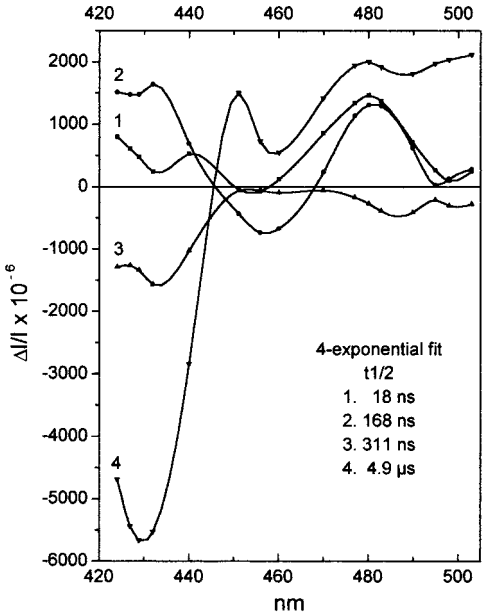

FIGURE 3: Spectra (423−500 nm) of the different kinetics components involved in the flash-induced spectral changes in the 0−30 μs time range deconvoluated with a 4-exponential function of the S52 mutant: saturating flashes, 0.9 s apart.

mexfit assuming a 4-exponential function (see Materials and Methods). In the control experiment (Figure 3), the computed half-times are 18 ns, 168 ns, 311 ns and 4.9 μs for spectra 1−4, respectively. In the presence of FCCP which collapses

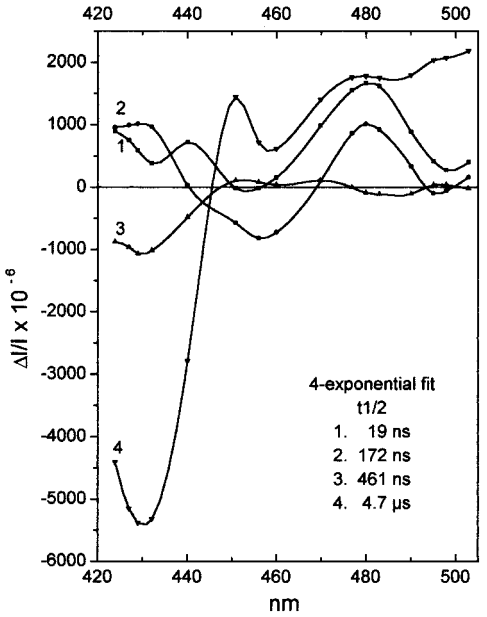

FIGURE 4: Same as Figure 3, in the presence of 8 μM FCCP.

the permanent membrane potential (Figure 4), the half-times are 19 ns, 172 ns, 461 ns, and 4.7 μs, respectively, i.e., very close to those measured in the control experiment (Figure 3). One can conclude that the process of electron transfer within PS I centers is little or not dependent on the value of the permanent delocalized membrane potential. The similarity of the two sets of spectra illustrates the robustness of the deconvolution procedure. The spectra of the kinetics components with half-times of ∼18 and ∼170 ns display the same characteristic absorption bands in the 450−500 nm range ascribed to the electrochromic shift induced by A_1^- and already seen in spectrum 1, Figure 2. This suggests that the oxidation of phylloquinone is biphasic. There are nevertheless reproducible differences between the two spectra such as the small absorption bands seen in the 420−440 nm range. The ∼5 μs component displays a spectrum close to that of ($P700^+$−P700) difference spectrum (*18*). A similar half-time for the reduction of $P700^+$ has been reported by Delosme (*19*) in the case of S52 mutant. The data used in Figures 3 and 4 have been fitted by the program mexfit with a 3-exponential function (not shown): the three components obtained have spectra close to spectra 1, 2, and 4, Figures 3 and 4, with half-times around 20 ns, 150 ns, and 4 μs, respectively.

In Figures 3 and 4, the ∼400 ns component shows a negative peak around 430 nm which could be tentatively ascribed to the electron transfer from an iron−sulfur center (F_X, F_AF_B) to ferredoxin. The oxidation of any of these iron−sulfur centers, F_X and F_AF_B, is associated with the disappearance of a wide negative band peaking around 430 nm (X430 (*20*)). Conversely, the reduction of ferredoxin is associated with a negative absorption band with a deacreasing amplitude from 420 to 500 nm. According to Sétif (personal communication), the extinction coefficients associated with the oxidation of the iron−sulfur clusters and the reduction of ferredoxin are both around 4.5 mM^{-1} cm^{-1} at 460 nm. Then, spectrum 4 is in reasonable agreement with the difference between the spectra associated with the oxidation of F_AF_B and the reduction of ferredoxin. The half-time of ∼400 ns is close to that previously reported by Sétif and

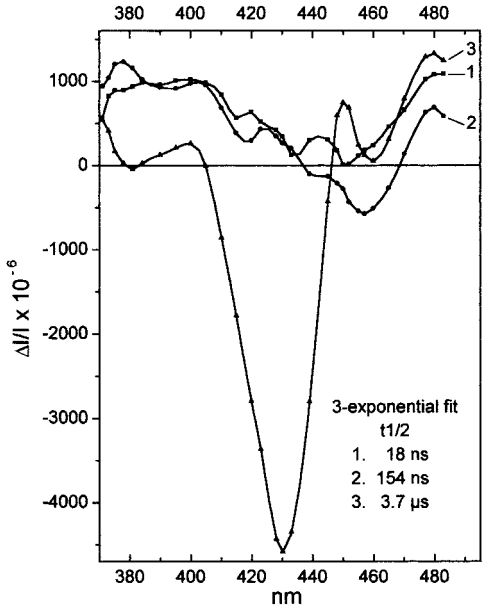

FIGURE 5: Spectra (371−485 nm) of the different kinetics components involved in the flash-induced spectral changes in the 0−30 μs time-range deconvoluated with a 3-exponential function of the S52 mutant: saturating flashes, 0.9 s apart; 8 μM FCCP.

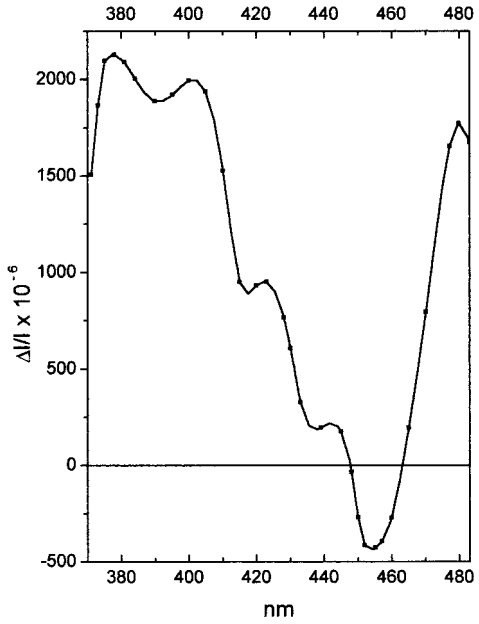

FIGURE 6: Difference spectrum associated with the oxidation of A_1^- and the reduction of an iron−sulfur cluster (F_X, F_AF_B?). Sum of spectra 1 and 2 shown in Figure 5.

Bottin (500 ns (*21*)). However, we consider that the ~400 ns component shown in Figures 3 and 4 is at the limit of accuracy of the deconvolution procedure and that a more refined analysis is required to reliably characterize the electron-transfer kinetics between iron−sulfur centers and ferredoxin.

In Figure 5, the kinetics of absorption changes have been measured at wavelengths between 371 and 485 nm. The data have been fitted with a 3-exponential function with half-times of 18 ns, 154 ns, and 3.7 μs for spectra 1−3, respectively. These values are close to those obtained in Figures 3 and 4. The spectra of the 18 and 154 ns components present large similarity but with some significant and reproducible differences, namely around 375, 417, and 438 nm. In Figure 6 is shown the sum of spectra 1 (18 ns) and 2 (154 ns) from Figure 5. The resulting spectrum is very likely associated with the transfer of one electron from phylloquinone to the iron−sulfur centers (F_X, F_AF_B). This spectrum displays a positive peak around 380 nm we ascribe to the semiphylloquinone A_1^- and the shift in the 450−480 nm range, already characterized in Figures 3 and 4.

We have analyzed the effect of a permanent membrane potential on the kinetics of A_1^- oxidation. In Figure 7 are shown the kinetics of the flash-induced absorption changes measured for the difference (481−457 nm). This wavelength difference corresponds to the peak and trough of the local electrochromic shift we ascribe to the presence of A_1^- (see Figure 2). In the control experiment, algae are illuminated by a saturating flash. In these conditions, the delocalized membrane potential induced by a full charge separation is superimposed to the permanent membrane potential induced by the hydrolysis of ATP. In a second experiment, algae, in the presence of FCCP, are illuminated by subsaturating flashes. In these conditions, the PS I centers are submitted to a much smaller transmembrane potential since (i) the permanent component is collapsed upon FCCP addition and (ii) only a part of the PS I reaction centers undergoes a charge

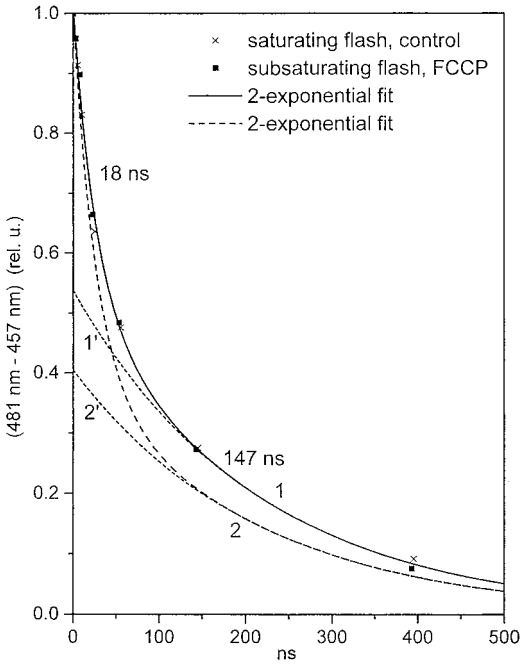

FIGURE 7: Kinetics of A_1^- oxidation, measured by the difference (481−457 nm). S52 mutant: (×) saturating-flash excitation, control; (■) subsaturating-flash excitation, hitting ~30% of PS I centers, 8 μM FCCP; curve 1, same 2-exponential fit of the 2 sets of data, after subtraction of the ~4 μs component; curve 1′, extrapolation to time zero of the 147 ns component; curve 2, theoretical 2-exponential function, computed for a value of *K* 1.7 time larger than for curve 1 (see Discussion); curve 2′, extrapolation to time zero of the slowest component of curve 2.

separation. After normalization of the amplitude of the signal, one can observe that both series of data can be fitted by the same 2-exponential function, with half-times of 18 and 147 ns, respectively. We conclude that the relative amplitudes and rate constants of the two phases ascribed to the oxidation of A_1^- are independent of the value of the delocalized membrane potential. Similar conclusions are drawn from experiment in Figure 8, performed at 377 nm. At this

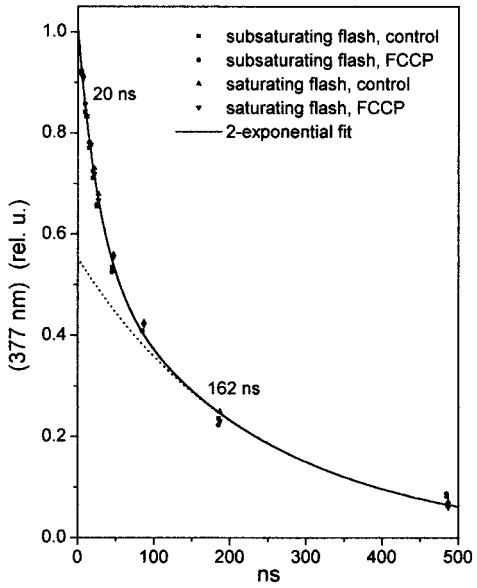

FIGURE 8: Kinetics of A_1^- oxidation, measured at 377 nm under saturating or subsaturating-flash excitation (hitting ~30% of PS I centers) ± 8 μM FCCP.

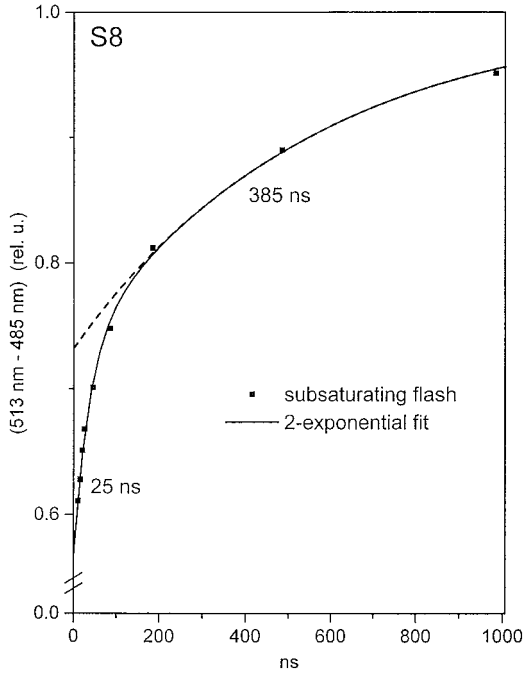

FIGURE 9: Kinetics of the slow increase of the delocalized membrane potential of S8 mutant: subsaturating flashes (hitting ~30% of PS I centers), 0.9 s apart; solid line, 2-exponential fit; dashed line, extrapolation to time zero of the 385 ns component.

wavelength, the amplitude of the ~4 μs component is negligible (see Figure 5) and the absorption changes exclusively reflect A_1^- oxidation. After normalization, all the data are fitted with the same 2-exponential function with half-times of 20 and 162 ns, respectively.

In Figure 9, the kinetics of formation of the delocalized membrane potential in mutant S8 with a normal chlorophyll antenna content has been measured as the difference (513−485 nm) to cancel the signal associated with the local electrochromic shift characterized in Figure 2. S8 mutant has been submitted to repetitive subsaturating-flash excitation; under these conditions, most of the excitons are trapped by P700 and the carotenoid triplet formation is minimized (*22*).

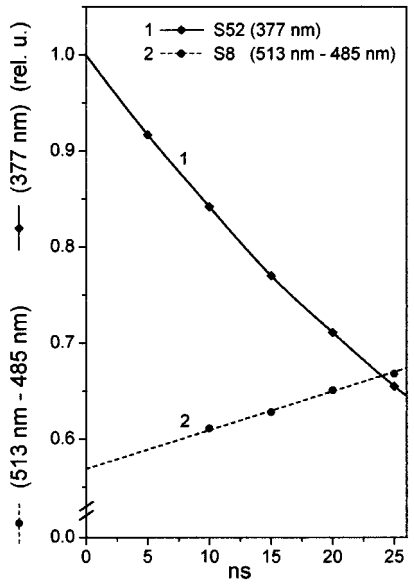

FIGURE 10: Kinetics of A_1^- oxidation (curve 1, data from Figure 8) and of the membrane potential increase (curve 2, data from Figure 9) in the −25 ns time range.

The amplitude of the signal has been normalized to the amplitude measured at 30 μs so that the full electrogenicity associated with PS I turnover is measured. At this time, for each excited PS I center, a negative charge has crossed the membrane from the lumen to the stroma. The kinetics of the membrane potential increase displays a first phase, not resolved here and completed in less than 10 ns, very likely associated with the transfer of one electron from P700 to A_1 (amplitude ~ 0.57, Figure 10, curve 2). In Figure 9, the solid line corresponds to the 2-exponential fit with half-times of 25 and 385 ns and amplitudes of 0.16 and 0.27, respectively. Upon a saturating-flash excitation (not shown), the corresponding half-times are 21 and 234 ns with amplitudes of 0.18 and 0.23, respectively. We assume that the multiphasic increase reflects the electron transfer from A_1 to the stroma. The few hundreds of ns component is never correctly fitted by a one-exponential function, but the attempt to fit with a larger number of exponentials leads to nonreproducible results from one batch to the other. We conclude that the increasing phase of the membrane potential always includes a component with a half-time close to that of the ~20 ns oxidation phase of A_1 and a multiphasic slower phase, with half-times longer than that of the ~160 ns oxidation phase of A_1^-.

DISCUSSION

The kinetics of A_1^- oxidation has been measured in the absorption band of A_1^- in the near UV and by the electrochromic shift of a carotenoid pigment induced by the negative charge on A_1. The spectrum of this electrochromic shift (Figure 2, spectrum 3) has been corrected for the increase of the delocalized membrane potential. We confirm that A_1^- oxidation is a biphasic process. The relative amplitudes and half-times of the two kinetics components are similar when measured at 377 nm or by the difference (481−457 nm). These half-times are close to those reported for spinach chloroplasts PS I centers (*5*). We do not observe in *Chlorella* the fast component ($t_{1/2}$ ~ 7 ns) reported by Brettel (*8*) in *Synechocystis* PS I centers. Two classes of hypotheses can be proposed to interpret the biphasic oxida-

tion of A_1^-:

Hypothesis 1 (As Proposed in Refs 7 and 8). It is assumed that the equilibrium constant K between A_1 and F_X is close to 1. The sequence of events is:

$$A_1^- + F_X^+ \underset{k_2}{\overset{k_1}{\rightleftharpoons}} A_1 + F_X \quad (1)$$

$$F_X + F_AF_B^+ \xrightarrow{k_3} F_X^+ + F_AF_B \quad (2)$$

with $k_1 \cong k_2$ and $k_3 < k_1$.

In this hypothesis, the redox equilibrium in reaction 1 is reached with a half-time ~20 ns, proportional to $1/(k_1 + k_2)$. The slower phase ($t_{1/2} \sim 160$ ns, proportional to $1/k_3$) is associated with the decay of this quasi equilibrium state by electron-transfer toward F_AF_B. Two lines of evidence argue against hypothesis 1:

(1) Leibl et al. (*10*) determined the kinetics and amplitude of the electrogenic phase associated with the electron transfer within PS I centers by measuring the photoelectric response of oriented PS I membranes extracted from *Synechocystis*. After a selective extraction of F_AF_B, the authors measured a half-time of 167 ns for reaction 1. This value is close to the one reported here for the slow component of A_1^- oxidation. This contradicts hypothesis 1 according to which the ~160 ns component is associated with reaction 2.

(2) A potential applied between A_1 and F_X will induce a shift of the equilibrium constant $K = k_1/k_2$ provided that the A_1^- to F_X^+ electron transfer is electrogenic. In intact cells of *Rhodopseudomonas viridis*, Baymann and Rappaport (*23*) reported that the equilibrium constant of the electron transfer between the primary donor and cytochrome c_{559} is increased by a factor 3 upon addition of FCCP which collapses the permanent electrochemical proton gradient induced by the hydrolysis of ATP. Taking into account that the dielectrically weighted distance between the primary donor and cytochrome c_{559} is ~0.15, the estimated value of the permanent membrane potential is $(\log 3 \times 60 \text{ mV})/0.15 \cong 190$ mV. It is worth noting that in bacteria, unlike in algae (*12*), the osmotic component of the electrochemical proton gradient is negligible. In S52 mutant, the permanent membrane potential has been estimated to ~30 mV (*11*) and represents only a part of the electrochemical proton gradient associated with the hydrolysis of ATP. On the other hand, the membrane potential increase induced by a saturating-flash excitation can be estimated to ~30 mV (*24*), which leads to an overall value of ~60 mV and the potential applied between A_1 and F_X is 60 mV $\times$ E_{AF} in which E_{AF} is the dielectrically weighted distance between A_1 and F_X.

Experimental Determination of E_{AF}. In Figure 10 are shown on an expended time scale the kinetics of A_1^- oxidation using S52 mutant and that of the rise of the transmembrane electrical potential using S8 mutant, both measured after a subsaturating-flash excitation in the presence of uncoupler. The initial rate r_1 of A_1^- oxidation is proportional to the initial slope of curve 1. The initial rate r_2 of the membrane potential rise associated with the transfer of electron from A_1^- to F_X is proportional to the initial slope of curve 2. According to hypothesis 1, r_1 is proportional to k_1 and independent of k_2 and k_3. We have $r_2 = r_1E_{AF}$ and $E_{AF} = r_2/r_1$. From Figure 10, we have computed E_{AF} equal to 0.27.

Scheme 1

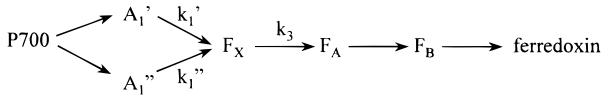

We conclude that the electrical potential applied between A_1 and F_X after a saturating flash-excitation (control) is ~60 mV $\times$ 0.27 = ~16 mV. After a subsaturating flash-excitation, hitting ~30% of PSI centers and in the presence of uncoupler, this potential is ~10 mV $\times$ 0.27 = ~3 mV. If K_S is the value of the equilibrium constant of reaction 1 after a saturating flash and K_W that after a weak flash, one has $K_S/K_W = 10^{(16-3)/59} = 1.7$ in which 59 mV = ln 10 $\times$ RT/F. In Figure 7 we have computed, on the basis of hypothesis 1, the predicted kinetics of A_1^- oxidation after a subsaturating-flash excitation (curve 2), assuming that curve 1 is the kinetics after the saturating-flash excitation. The difference between curve 1 and curve 2 is more than 5 times larger that the experimental error. Similar conclusions can be drawn from Figure 8. It is worth pointing out that in the previous paragraphs we had very likely underestimated the value of the permanent membrane potential, which is higher under repetitive-flash excitation which induces ATP synthesis than in dark-adapted material (*11*). The absence of any significant effect of the membrane potential on the relative amplitude of the two phases of A_1^- oxidation led us to consider hypothesis 1 as unlikely.

Hypothesis 2. There are two classes of phylloquinones which differ by their oxidation rate constants k_1' and k_1''. The absence of effect of the membrane potential on the relative amplitude of the two phases of phylloquinone oxidation implies that K is high, i.e., that k_1' and $k_1'' \gg k_2$. Several structural hypotheses can account for the data: (1) The native photosynthetic membrane includes two types of PS I centers at equivalent concentration. This hypothesis seems to us quite unlikely as we obtain reproducible results in terms of the half-times and relative amplitudes of the two kinetics components, comparing different batches of algae, different mutants, or different species (*Chlorella* and *Chlamydomonas* (not shown)). (2) Photosystem I is present under two conformational states which differ by the rate of A_1^- oxidation. The equilibrium constant between these two states is close to 1, and the rate of equilibration is slower than the rate of A_1^- oxidation. Alternatively, the active phylloquinone may have two different localizations in the reaction center. (3) The two chains of electron carriers associated with the heterodimer forming the PS I center are supposed to be both active. This hypothesis is summarized in Scheme 1.

Scheme 1 takes into account recent information deduced from photoelectric measurements (*25*, *26*) which suggest that F_B is the terminal iron−sulfur acceptor in PsaC polypeptide. To account for the similar amplitude of the two phases of A_1^- oxidation, we assume that the electron-transfer reactions from P700 to A_1' and to A_1'' have similar rate constants. Thus, the probability of electron transfer from P700 to A_1' and A_1'' is about the same (~0.45 for the A_1' branch and ~0.55 for the A_1'' branch). On the other hand, the oxidation rate constant of $A_1'^-$ is about 8 times larger than that of $A_1''^-$. The rate constants are $k_1' = \ln 2/(20 \times 10^{-9}) = 3.5 \times 10^7$ s^{-1} and $k_1'' = \ln 2/(160 \times 10^{-9}) = 4.4 \times 10^6$ s^{-1}, respectively.

The 25 ns component in the membrane potential rise (Figure 9) is associated with the electrons transferred via the A_1' pathway (0.45 of the total). As the amplitude of the 25 ns component is 0.16, these electrons span 0.16/0.45 = 0.36 of the dielectrically weighted distance of P700 to the stroma. This is larger than expected from the crystallographic structure of PS I centers (*27*). We thus conclude that the 25 ns phase is associated with the electron transfer from A_1' to F_A which implies that k_3 is larger than k_1'. Leibl et al. (*10*) arrived to similar conclusions on the basis of photoelectric measurements. The dielectrically weighted distance we assume for A_1' (or A_1'') to F_A (0.36; see above) is lower than the amplitude of the slow membrane potential rise (0.43; Figure 9) associated with the electron transfer from A_1^- to the lumen. If one takes into account that the electron transfer from F_B to ferredoxin is very likely electrically silent (*25*, *26*), the difference (0.07) is possibly associated with the electron transfer from F_A to F_B which would account for the "tail" of the electrogenic phase. This implies that the half-time for the electron transfer between F_A and F_B is in the several hundreds of nanosecond time range.

The quasi equality of the amplitude of the two kinetics components in A_1^- oxidation suggests that A_1' and A_1'' occupy a quite symmetrical position with respect to P700. Structural perturbations induced by the procedure of extraction or purification could modify the relative rate of the P700 to A_1' or A_1'' reaction, yielding to changes in the relative amplitude of the two components. It is worth pointing out that the two phylloquinones differ in their extractability by organic solvents (*28*, *29*). The activity is lost only when both quinones are extracted. In the case of isolated centers, the variability in the relative amplitude of the two kinetics components of A_1^- oxidation can possibly result from a partial extraction of the more loosely bound phylloquinone.

Some asymmetry in the relative localization of F_X with respect to A_1' and A_1'' could account for the difference between k_1' and k_1''. The fact that a similar carotenoid shift is associated with the reduction of A_1' and A_1'' suggests that two carotenoid pigments belonging to PsaA and PsaB are located in symmetrical positions with respect to A_1' and A_1'', respectively. On the other hand, an asymmetrical position of several pigments (chlorophylls?, carotenoids?) subjected to electrochromic shifts induced by $A_1'^-$ or $A_1''^-$ could account for the small differences observed in the spectra of the two kinetics components (Figures 3−5). This effect could reflect the asymmetry between PsaA and PsaB and favors the hypothesis depicted in Scheme 1.

The functional analysis of mutants perturbed in the vicinity of the phylloquinones binding sites, either on the PsaA or PsaB polypeptide, will be a privileged way to operate a choice between the different interpretations discussed in this paper.

ACKNOWLEDGMENT

F. Rappaport is acknowledged for critical reading of the manuscript and valuable discussions.

REFERENCES

1. Malkin, R. (1996) in *Oxygenic Photosynthesis: The Light Reactions* (Ort, D. R., and Yocum, C. F., Eds.) pp 313−332, Kluwer Academic Publishers, Dordrecht, The Netherlands.
2. Brettel, K. (1997) *Biochim. Biophys. Acta 1318*, 322−373.
3. Hecks, B., Wulf, K., Breton, J., Leibl, W., and Trissl, H.-W. (1994) *Biochemistry 33*, 8619−8624.
4. Golbeck, J. H. (1994) In *The Molecular Biology of Cyanobacteria* (Bryant, D. A., Ed.) pp 319−360, Kluwer Academic Publishers, Dordrecht, The Netherlands.
5. Mathis, P., and Sétif, P. (1988) *FEBS Lett. 237*, 65−68.
6. Brettel, K. (1988) *FEBS Lett. 239*, 93−98.
7. Sétif, P., and Brettel, K. (1993) *Biochemistry 32*, 7846−7854.
8. Brettel, K. (1999) in *Photosynthesis: Mechanisms and Effects* (Garab, G., Ed.) Vol. I, pp 611−614, Kluwer Academic Publishers, Dordrecht, The Netherlands.
9. Bock, C. H., van der Est, A. J., Brettel, K., and Stehlik, D. (1989) *FEBS Lett. 247*, 91−96.
10. Leibl, W., Toupance, B., and Breton, J. (1995) *Biochemistry 34*, 10237−10244.
11. Joliot, P., and Joliot, A. (1985) *Biochim. Biophys. Acta 806*, 398−409.
12. Finazzi, G., and Rappaport, F. (1998) *Biochemistry 37*, 9999−10005.
13. Lavergne, J., Delosme, R., Larsen, U. and Bennoun, P. (1984) *Photobiochem. Photobiophys. 8*, 207−219.
14. Béal, D., Rappaport, F., and Joliot, P. (1999) *Rev. Sci. Instrum. 70*, 202−207.
15. Joliot, P., Béal, D., and Rappaport, F. (1999) in *Photosynthesis: Mechanisms and Effects* (Garab, G., Ed.) Vol. 5, pp 4247−4252, Kluwer Academic Publishers, Dordrecht, The Netherlands.
16. Müller, K.-H., and Plesser, T. (1991) *Eur. Biophys. J. 19*, 231−240.
17. Grzybek, S., Baymann, F., Müller, K.-H., and Mäntele, W. (1993) in *Fifth International Conference On the Spectroscopy of Biological Molecules* (Theophanides, T., Anastassopoulou, J., and Fotopoulos, N., Eds.) pp 25−26, Kluwer Academic Publishers, Dordrecht, The Netherlands.
18. Hiyama, T., and Ke, B. (1972) *Biochim. Biophys. Acta 267*, 160−171.
19. Delosme, R. (1991) *Photosynth. Res. 29*, 45−54.
20. Hiyama, T., and Ke, B. (1971) *Arch. Biochem. Biophys. 147*, 99−108.
21. Sétif, P., and Bottin, H. (1994) *Biochemistry 33*, 8495−8504.
22. Wolff, C., and Witt, H. T. (1969) *Z. Naturforsch. 24b*, 1031−1037.
23. Baymann, F., and Rappaport, F. (1998) *Biochemistry 37*, 15320−15326.
24. Witt, H. T. (1979) *Biochim. Biophys. Acta 505*, 355−427.
25. Mamedov, M. D., Gourovskaya, K. N., Vassiliev, I. R., Golbeck, J. H., and Semenov, A. Yu. (1998) *FEBS Lett. 431*, 219−223.
26. Mamedova, A. A., Gourovskaya, K. N., Mamedov, M. D., Vassiliev, I. R., Golbeck, J. H., and Semenov, A. Yu. in *Photosynthesis: Mechanisms and Effects* (Garab, G., Ed.) Vol. I, pp 651−654, Kluwer Academic Publishers, Dordrecht, The Netherlands.
27. Schubert, W. D., Klukas, O., Krauss, N., Saenger, W., Fromme, P., and Witt, H. T. (1995) in *Photosynthesis: from Light to Biosphere* (Mathis, P., Ed.) Vol. 2, pp 3−10, Kluwer Academic Publishers, Dordrecht, The Netherlands.
28. Malkin, R. (1986) *FEBS Lett. 208*, 343−346.
29. Biggins, J., and Mathis, P. (1988) *Biochemistry 27*, 1494−1500.

BI990857C